INTERNATIONAL JOURNAL OF
COASTAL & OFFSHORE ENGINEERING
IJCOE Vol.4/No. 4/ Winter 2019 (1-8)

Available online at: http://ijcoe.org/browse.php?a_code=A-10-233-1&sid=1&slc_lang=en

Numerical Validation of Experimental Tests Conducted on a Fixed Offshore Oscillating Water Column

Milad Zabihi[1], Said Mazaheri[2*], Masoud Montazeri Namin[3]

[1] *Ph.D student, Iranian National Institute for Oceanography and Atmospheric Science; milad.zabihi@inio.ac.ir*
[2*] *A/Professor, Iranian National Institute for Oceanography and Atmospheric Science; said.mazaheri@inio.ac.ir*
[3] *Assistant Professor, University of Tehran; mnamin@ut.ac.ir*

ARTICLE INFO

Article History:
Received: 18 Sep. 2018
Accepted: 16 Feb. 2019

Keywords:
OWC
Numerical Simulation
Wave Energy
CFD
Experimental

ABSTRACT

Supplying world future energy is tied with renewable energies and wave energy is one of the biggest resources of renewable energy which is somehow untapped. Oscillating Water Column (OWC), one of the most familiar devices in harnessing wave energy, is still not being properly commercialized due to the complicated hydrodynamic behavior. Offshore OWCs are exposed to higher wave energy; however, the researches on this kind of OWCs is limited. Hence, in this paper, a fully nonlinear two phase flow model of a fixed offshore OWC is developed using Ansys Fluent. Unlike the previous studies, the developed numerical model has the merit of being validated against a relatively large scale physical model (1:15). The results of the model are compared by those obtained in experimental campaign conducted by the authors. Results of both free surface elevation and air pressure in the OWC chamber are compared. Generally, the results showed an admissible accordance between numerical and experimental model. Some discrepancies could be detected in the free surface elevation in the chamber especially for short wave period. This can be attributed to the increase of nonlinear effects in the chamber by increase of wave steepness. The developed model can be applied for further researches on OWCs such as optimization or improving OWC performance.

1. Introduction

Undoubtedly, supplying increasing energy demand is one of the biggest challenges in today's world. On the other hand, energies based on carbon emission will be finished soon in addition to their destructive impacts on our environment. Hence, renewable energy resources such as wind, solar, tidal and wave are non-pollutant appropriate options for replacement. Among different renewable energy resources, wave energy is an untapped resource which has the merit of relatively high energy density [1]. Of the numerous devices developed for harnessing wave energy [2], one that particularly stands out is Oscillating Water Column (OWC). An OWC consists of a partially submerged compartment which is open to sea at the bottom. Incident wave interaction with the compartment induces water fluctuation inside the chamber. The water fluctuation causes the air pressure in the chamber to be compressed or depressurized. Air flow generated by this mechanism can drive a turbine installed to the chamber and then using a generator electricity will be produced.

The OWCs can be constructed nearshore or offshore [3]. Offshore OWCs which are exposed to higher wave energy [4] and consequently result in higher energy capture. A lot of numerical and experimental researches have been conducted on OWCs in recent years. Numerical models developed for assessing the OWC performance can be classified into two main groups. The first are those studies based on potential flow theory which include the works done by [5]–[8]. Evans [5] considered the free surface fluctuation in the chamber as a rigid piston which is almost a sound assumption particularly for the cases with large ratios of wavelength to chamber width. Then, [6]–[9] upgraded the rigid piston model by introducing periodic surface pressure distribution and considering free surface curvature. Later, researchers used boundary element method to solve rigid piston model or models based on surface pressure distribution [10], [11]. Although computational cost for potential flow theory is not high, it has demerits such as having no capability in taking nonlinear interaction in to account. Hence, applying CFD approaches based on solving Navier-Stokes equation for considering nonlinear

interactions such as wave breaking or sloshing in the chamber is the second approach toward numerical simulation of OWCs. Given the ongoing progress in CFD models and computers' process ability, it seems that CFD is the most appropriate tool for modeling WECs such as OWCs. A number of efforts have been performed to model OWCs using numerical wave tank (NWT) and applying Navier-Stokes equation. Iturrioz et al. [12] used Open Foam incompressible two phase flow to model OWC-wave interaction. Vyzikas et al. [13] and Simonetti et al. [14], [15] also applied Open Foam and validated their two dimensional incompressible model against their experimental data. Reef3D was another code developed for OWC simulation by Kamath et al. [16]. They validated their model against bottom standing OWC experiments conducted by Morris Thomas et al. [17].

Lou et al. [18] performed a nonlinear analysis on the efficiency of fixed OWC for fully nonlinear waves using Ansys Fluent. The key result of that research was a substantial decrease in the hydrodynamic efficiency of the OWC device with increasing wave height. Anbarsooz et al. [19] conducted such a similar study and evaluated steep wave effects on the performance of a fixed OWC using Ansys Fluent.

Very recently, Elhanafi et al. [20]–[23] did a thorough job on both bottom fixed and bottom detached OWCs. They used Star-CCM+ to develop their CFD models. They evaluated energy balance in offshore [24] and onshore OWCs [25] and investigated the effects of asymmetric back and forth walls on efficiency of the offshore OWCs [20].

Although a lot of studies have been conducted on OWCs, there are steps toward commercializing the device perhaps due to the complicated hydrodynamic behavior of an OWC. Numerical models are great tools to bridge this gap as they need much less budget. The literature review indicates that a huge part of the previous studies is devoted to onshore or shore-based OWCs and less work has been done on offshore OWCs. Hence the aim of this paper is to validate the fully nonlinear model for an offshore OWC-wave interaction. Without validation it is impossible to assess the model accuracy and suitability. Unfortunately, accessibility to experimental data in the current issue is hard due to the limited experimental tests. Therefore, for validation of the current model, experimental tests performed by the authors have been used. It should be mentioned that the tests have the advantage of being relatively large scale experiments (Scale 1:15).

The rest of the paper can be summarized as follows; in section 2 a description of the experimental tests which have been used for validation is presented. Section 3 is devoted to numerical simulation where governing equations, boundary conditions and all relevant numerical settings are presented. Section 4 compares the results obtained by numerical procedure with those measured in experimental campaign. Section 5 is a brief summary of the current research which ends up with concluding remarks.

2. Description of the Experiments

Experimental tests were carried out at National Iranian Marine Laboratory (NIMALA), Tehran, Iran. The Laboratory is equipped with a towing tank of 400 m length, 6 m width and 4 m depth. The wave generator system which is a piston type wave maker can be set up to produce both regular and irregular waves. The regular wave height can reach to 50 cm height and 3 s period. The system is capable of generating different types of irregular wave spectra bounded to significant wave height 40 cm and peak period 3 s. At the end of the tank there is a dissipating beach to prevent reflection from the end wall of the tank. Moreover, Due to the long length of the wave tank interference of the reflected wave and incident wave is not a challenge so that the obtained results showed accurate incident wave generation. As stated before, 1:15 scale of a fixed offshore OWC was built using plexiglass material. The thickness of the material used for building OWC was 1cm except for the front wall which was 1.4 cm to decrease the risk of front wall distortion due to the wave action. To keep OWC in its position and to prevent any wave induced movement, a steel holding frame was designed which is shown in Figure 1. As can be seen, the OWC is placed exactly in the middle of the tank in order to minimize the side wall effects.

Figure 1. 3D view of holding frame for keeping OWC in its position [26]

Length, width and height of the OWC is shown in Figure 2. Further details about how OWC device dimensions were determined can be found in Ref. [27]. There are several ways for simulating Power Take Off (PTO) and its relevant damping; however, in this paper, as can be seen in Figure 2, slot shaped aperture is used to simulate PTO damping. For the test series used for validation, slot size (S=0.5 cm) was used. This value was selected according to previous results which showed that aperture ratio (the ratio of slot area to the chamber roof area) of 0.6 to 0.7% performs optimal.

Water depth (d=4 m) and front wall draft (Dr=20 cm) were also kept constant for validation tests. The wave tank longitudinal section is shown in Figure 3. Figure 3 also indicates the locations of the instruments such as Wave Gauges (WG) and Pressure Sensors (PS) installed in the chamber and along the wave tank. All data acquisition processes were performed at 50 Hz. Regular wave was introduced into the wave maker with constant wave height of H=15 cm and three different wave periods including T=1.8, 2 and 2.2 sec.

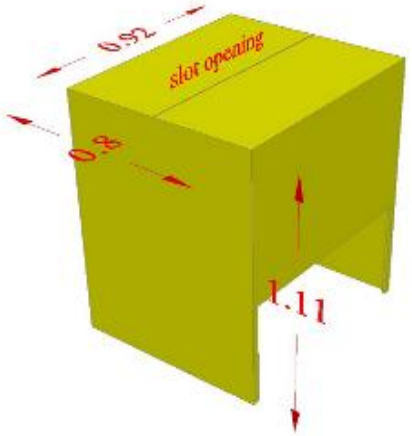

Figure 2. Dimensions of the physical model (meter) [27]

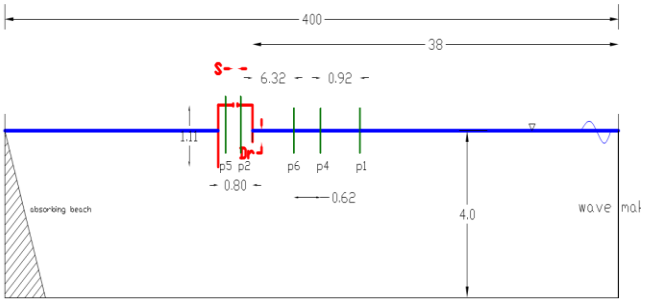

Figure 3. The Locations of the wave gauges and pressure sensors (Not to scale)

3. Numerical Simulation

3.1. Governing Equations

Fully nonlinear model based on Reynolds Averaged Navier Stokes (RANS) equation accompanied by Volume of Fluid (VOF) surface capturing method are the governing equations. Fluent solves Navier-Stokes and Continuity equation. Navier-Stokes equations in three dimensional coordination are as follows;

$$\frac{\partial u}{\partial t}+u\frac{\partial u}{\partial x}+v\frac{\partial u}{\partial y}+w\frac{\partial u}{\partial z}= -\frac{1}{\rho}\frac{\partial p}{\partial x}+g_x+\upsilon\left(\frac{\partial^2 u}{\partial x^2}+\frac{\partial^2 u}{\partial y^2}+\frac{\partial^2 u}{\partial z^2}\right) \quad (1)$$

$$\frac{\partial v}{\partial t}+u\frac{\partial v}{\partial x}+v\frac{\partial v}{\partial y}+w\frac{\partial v}{\partial z}= -\frac{1}{\rho}\frac{\partial p}{\partial y}+g_y+\upsilon\left(\frac{\partial^2 v}{\partial x^2}+\frac{\partial^2 v}{\partial y^2}+\frac{\partial^2 v}{\partial z^2}\right) \quad (2)$$

$$\frac{\partial w}{\partial t}+u\frac{\partial w}{\partial x}+v\frac{\partial w}{\partial y}+w\frac{\partial w}{\partial z}= -\frac{1}{\rho}\frac{\partial p}{\partial z}+g_z+\upsilon\left(\frac{\partial^2 w}{\partial x^2}+\frac{\partial^2 w}{\partial y^2}+\frac{\partial^2 w}{\partial z^2}\right) \quad (3)$$

where, u, v and w are components of velocity field in x, y and z direction, respectively. P is the pressure and ρ is density. υ is the kinematic viscosity and g_x, g_y and g_z are the gravitational acceleration components. However, assuming z is in gravity direction, g_x and g_y are equal to zero and g_z will be equal to $-g$.

Eq. (4) presents the continuity equation and Eq. (5) shows the continuity equation for incompressible flow.

$$\frac{\partial}{\partial x}(\rho u)+\frac{\partial}{\partial y}(\rho v)+\frac{\partial}{\partial z}(\rho w)+\frac{\partial \rho}{\partial t}=0 \quad (4)$$

$$\frac{\partial u}{\partial x}+\frac{\partial v}{\partial y}+\frac{\partial w}{\partial z}=0 \quad (5)$$

All parameters have been introduced following the Navier-Stokes equation.

As in this study it is focused on wave generation and its interaction with OWC, consequently free surface capture is an indispensable part of this study. Hence, for free surface tracking VoF method has been used. Hirt [28] developed the VOF method to solve the two-phase problem. The VOF formulation is based on the fact that two or more phases are immiscible. In each control volume, sum of the volume fraction of all phases is unit (Eq. (6)). If the q^{th} fluid volume fraction is recognized as α_q, then depending on α_q value the following three conditions are possible: α_q =0 shows that the volume is empty of q^{th} fluid, α_q =1 shows that the volume is full of q^{th} fluid and any other value between 0 and 1 shows the interface. The volume fraction is as follows;

$$\sum_{q=1}^{n}\alpha_q=1 \quad (6)$$

$$\frac{\partial}{\partial t}(\alpha_q)+\nabla.(\alpha_q\vec{v_q})=0 \quad (7)$$

where $\vec{v_q}$ is velocity vector.

3.2. Computational Fluid Domain and Boundary Conditions

The most important part of wave structure hydrodynamic study is to generate accurate waves. Simulation of a Numerical Wave Tank (NWT) is explained in this section (See Figure 4). The fluid domain of the numerical wave tank is of 50 meter length equal to approximately 8L (L= wavelength). One wave length at the far end of the NWT is devoted to damping zone to prevent unwanted reflection from outlet boundary.

For numerical wave generation, one may simulate wave paddle as a moving boundary and introduce the motion of the wave to the wave paddle. As this method involves dynamic mesh and needs remeshing in each time step, it may need much more efforts. However, Ansys Fluent has the capability to generate waves with a built-in function via velocity inlet wave boundary condition. No slip wall boundary condition is assigned to the bottom of the NWT. Other NWT boundary conditions include applying atmospheric pressure to the boundary which is above still water level and assigning an outlet condition to the NWT right hand boundary (See Figure 4).

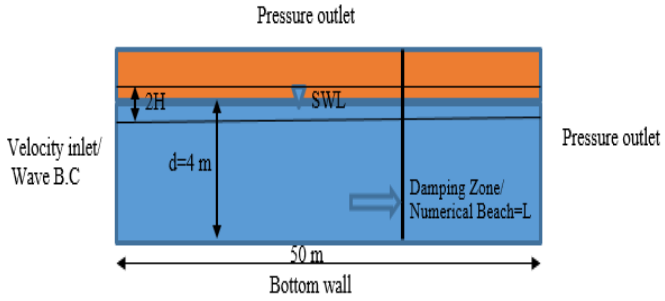

Figure 4. Schematic of the numerical wave tank

To capture wave propagation accurately, 3 types of mesh discretization has been applied for NWT developing. They are presented in Table 1. It should be noted that x is in the wave propagation direction while z is in the wave height direction. "H" stands for wave height and a zone equal to 2H has been refined for tracking wave height (Figure 4). Outside the wave propagation zone (2H), the grids are coarser. For grids in z direction, bias growth rate 1.2 was used meaning that each cell is 1.2 times bigger than its neighbor cell in z direction. This procedure was replicated for damping zone to help the wave dissipation more.

Time step size T/1000 to T/400 (T is wave period) leads to proper results according to previous studies recommendations [29]. Ansys Fluent allows any manipulation in time step size during simulation. Considering this feature, no significant change in wave generation results was observed by applying different time step sizes (in the aforementioned range). Hence, time step T/400 was selected for the following simulations.

Table 1. Three different mesh types discretization

Mesh Type	Delta x	Delta z
1	L/20	H/10
2	L/30	H/15
3	L/40	H/20

3.3. Numerical Settings in Ansys Fluent and NWT Result

For solving the governing aforementioned equations, the following numerical settings were applied. Considering pressure based solver, PISO scheme was applied for decoupling pressure velocity coupling. The spatial derivatives in the momentum equations were discretized using a second order upwind scheme and also a second order implicit formulation was applied for the time-derivatives. For VOF schemes, fluent presents two scheme called Modified-Hric and Compressive. According to Ansys Fluent user guide, Compressive scheme captures free surface more accurate. Hence, Compressive scheme was applied in this paper. The pressure interpolation method was based on PRESTO (PRE Staggering Option) scheme which is a widely used scheme for free surface modeling and wave generation models. The two equation turbulence model of k-w SST was applied to close the RANS equation.

The result of simulated wave propagation for a case with 15cm wave height and 2s period was compared against what was obtained from stokes second order wave theory (Figure 5). It should be mentioned that t/T is a dimensionless parameter showing the ratio of simulation time to the incident wave period. Although all of the tested mesh types yielded good results, the results showed that Mesh type 3 yields more accurate wave height with less than 0.04% error. Hence, Mesh type 3 is selected for the wave-OWC interaction in the following section.

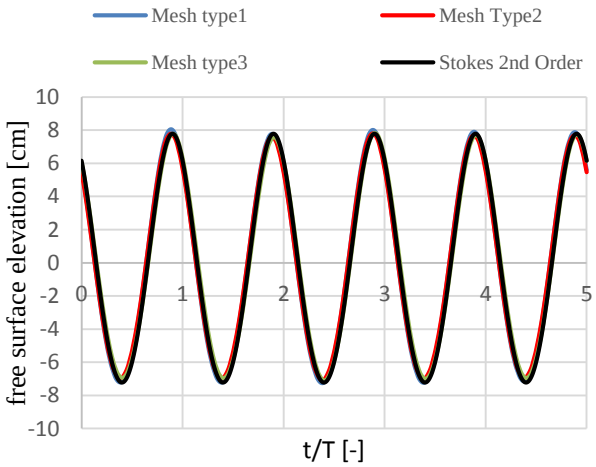

Figure 5. free surface elevation against nondimensional time; comparing three different discretization and Stokes 2nd order theory

4. Numerical Validation for an Offshore OWC

4.1. Model set up

In this section, the NWT model simulated in the previous section was developed for OWC-wave interaction. It is worth mentioning that all previous numerical settings were applied for this section. The mesh used for OWC-wave interaction is shown in Figure 6. The free surface mesh type was the same as mesh type 3.

The OWC position was according to Figure 1. However it should be noted that for reducing simulation run, half width of the OWC structure was considered by applying symmetry boundary condition. Moreover, in laboratory the distance between the OWC model and side walls was 2.54 but in the current

numerical model this was decreased to 1m for lowering the computation time.
The mesh size around the OWC structure was 0.01m and it was considered to be 0.0025m in the slot aperture. NWT in y direction was divided to six elements.

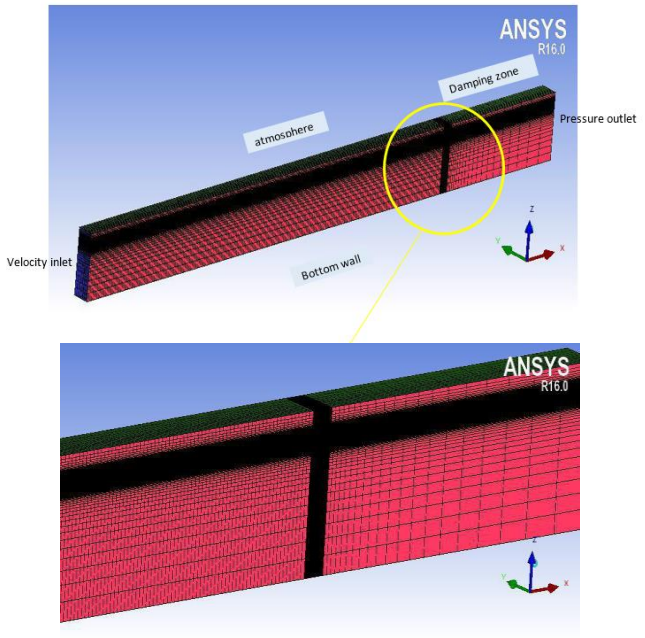

Figure 6. Mesh and boundary conditions used for OWC wave interaction; mesh refinement in free surface area and OWC position

4.2. Comparing numerical and experimental results

In this section the numerical results are compared with those observed in experiments. Wave height was kept constant at H=15 cm and three different values were considered for wave period (T=1.8, 2 and 2.2 s).
In the first step, the results are presented for free surface elevation outside the chamber (See
Figure 7-9). It should be noted that the results are presented for 5 wave cycles. The numerical results are in good agreement for the three probes located outside the chamber ensuring there is no unwanted reflection in numerical domain regardless of reducing the numerical tank width and length relative to experimental wave tank.
To evaluate the performance of numerical wave dissipation, the result of free surface elevation at the far end of the tank; that is to say x=50m, is presented in Figure 10. As it is clear, water depth fluctuation at simulation time greater than 2s is around 0.5cm which is a negligible value ensuring appropriate function of the dissipation zone.

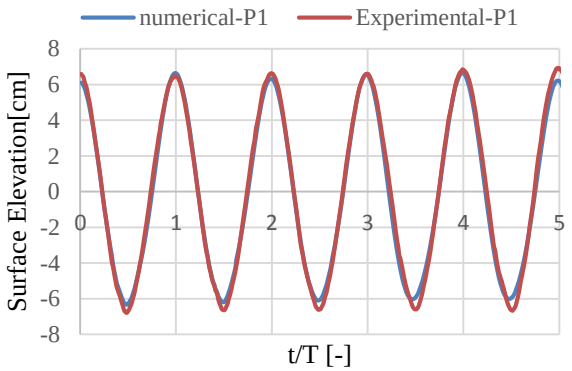

Figure 7. Free surface elevation at probe 1; numerical values versus experimental measurements (H=15 cm, T=2 s)

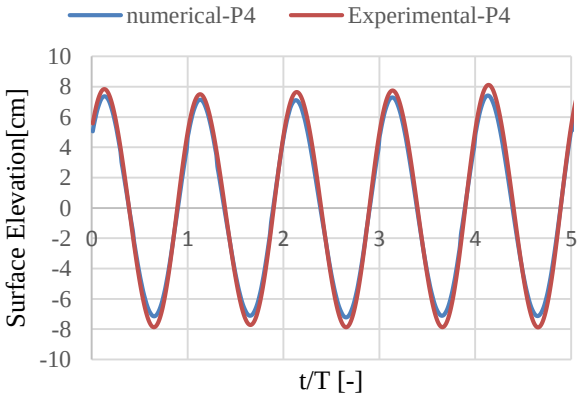

Figure 8. Free surface elevation at probe 4; numerical values versus experimental measurements (H=15 cm, T=2 s)

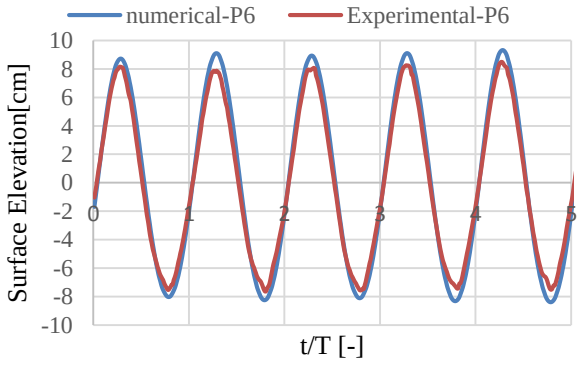

Figure 9. Free surface elevation at probe 6; numerical values versus experimental measurements (H=15 cm, T=2 s)

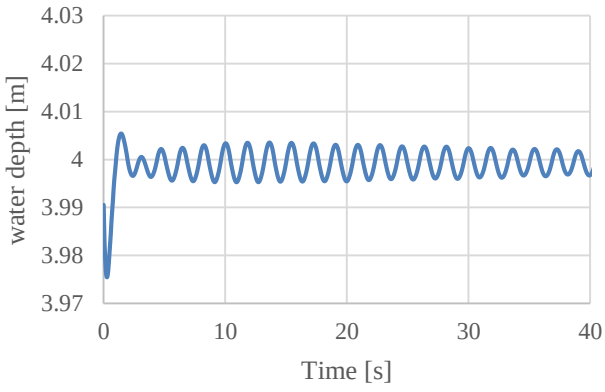

Figure 10. Numerical free surface elevation at x=50m

The numerical results corresponding to probes inside the chamber (P2 and P5) were compared with experimental measurements through Figure 11-12. Unlike the outside probes, for inside probes (P2 and P5) nonlinear interaction is more visible. Although there are some discrepancies especially for P2 at wave troughs, the numerical model could capture the nonlinearity in a good way.

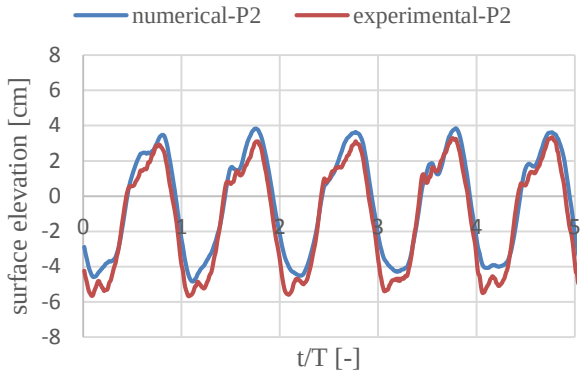

Figure 11. Free surface elevation at probe 2; numerical values versus experimental measurements (H=15 cm, T=2 s)

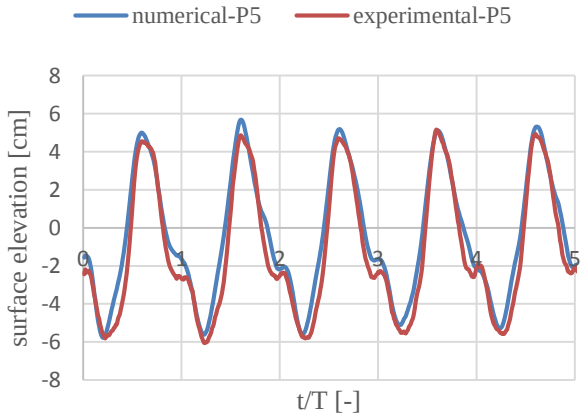

Figure 12. Free surface elevation at probe 5; numerical values versus experimental measurements (H=15 cm, T=2 s)

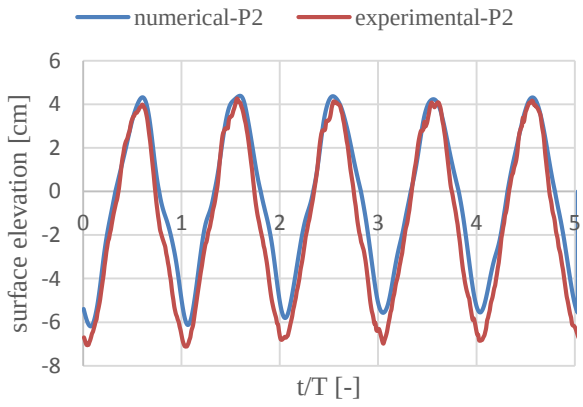

Figure 13. Free surface elevation at probe 2; numerical values versus experimental measurements (H=15 cm, T=2.2 s)

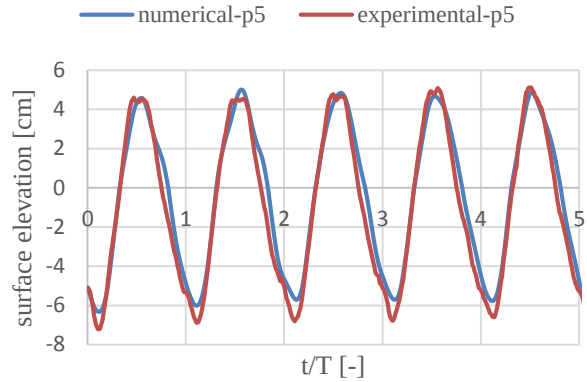

Figure 14. Free surface elevation at probe 5; numerical values versus experimental measurements (H=15 cm, T=2.2 s)

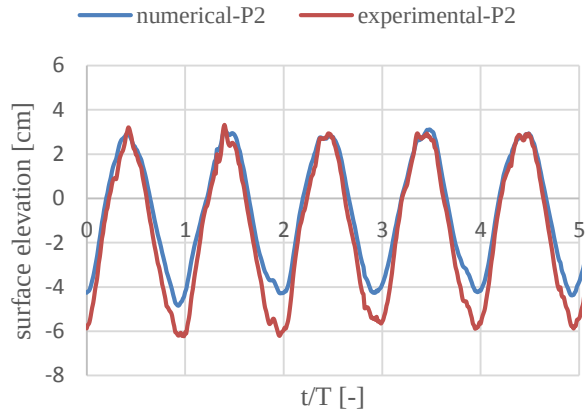

Figure 15. Free surface elevation at probe 2; numerical values versus experimental measurements (H=15 cm, T=1.8 s)

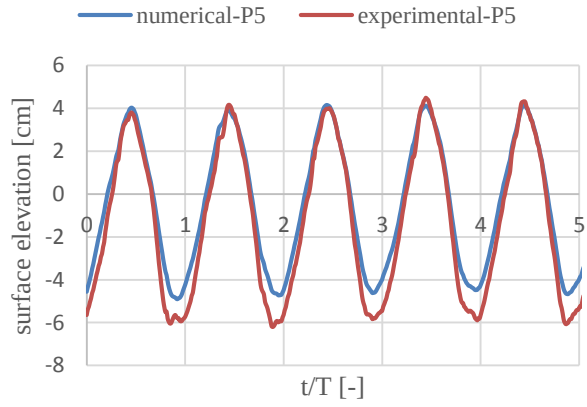

Figure 16. Free surface elevation at probe 5; numerical values versus experimental measurements (H=15 cm, T=1.8 s)

The aforementioned procedure was replicated for T=2.2s and T=1.8s. For abridgment, the results of the waves outside the chamber are not presented for T=1.8s and T=2.2s and just the inner chamber fluctuations are presented through Figure 13-16. As it is obvious, the results are in better agreement with experimental measurements for T=2.2s rather than T=1.8. This can be attributed to the higher wave steepness caused by lower wave period which consequently resulted in higher nonlinearity. Considering authors visual observation, this nonlinear interaction is mainly caused by sloshing phenomenon. In fact, short period waves

entering OWC may reflect from the chamber rear wall and interact with incoming wave at a location in the middle of the chamber. This will prevent free surface elevation in the chamber to have a piston shape fluctuation.

Chamber air pressure was another parameter evaluated in this paper as it is crucial to determine the chamber pressure to assess the OWC efficiency. The results of air pressure are presented in Figure 17 and 18. Admissible agreement can be detected between numerical results and experimental measurements. Although there are discrepancies in minimum and maximum pressure occurred in the chamber, the general pattern was captured by developed numerical model.

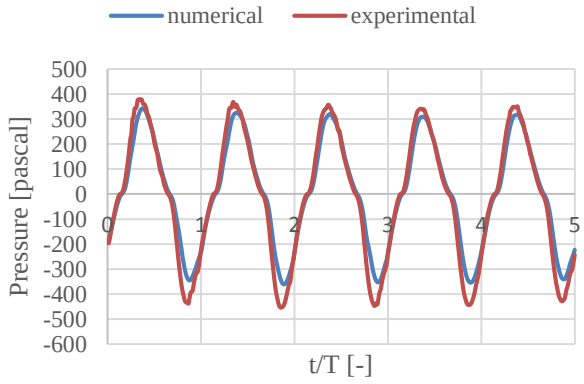

Figure 17. Chamber air pressure (T=1.8 s)

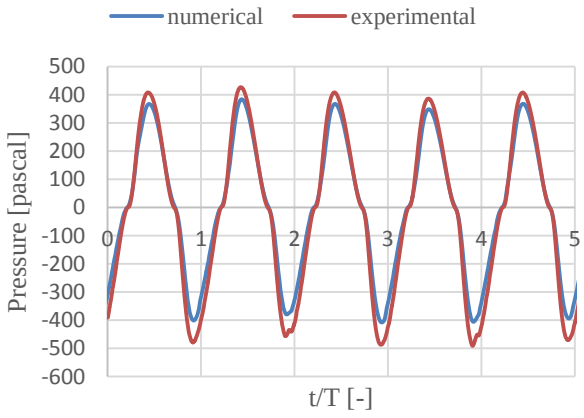

Figure. 18 Chamber air pressure (T=2.2 s)

5. Summary and Conclusions

OWC is one of the wave energy devices even attained full scale prototype but not fully commercialized yet. Surely, its performance should be optimized prior to commercializing the device and this needs further numerical and experimental researches. In this paper, a numerical model was developed using Ansys Fluent based on fully nonlinear two phase flow model. The free surface fluctuation outside and inside the chamber as well as air pressure inside that were compared with experimental results obtained by the authors, very recently. Generally, numerical results showed good accordance with experimental data especially for long waves (T=2 and 2.2 s) when the ratio of wave length to chamber length was large enough to act as a piston type oscillation. For short period wave; highly steep wave, some discrepancies between numerical and experimental results were observed inside the chamber. The developed model can be employed for further analyzes such as optimization of the OWC performance.

6. References

1- Khan, N., Kalair, A., Abas, N. and Haider, A., (2017), *Review of ocean tidal, wave and thermal energy technologies*, Renewable and Sustainable Energy Reviews. Vol.72, p.590–604. https://doi.org/10.1016/j.rser.2017.01.079

2- López, I., Andreu, J., Ceballos, S., Martínez de Alegría, I. and Kortabarria, I., (2013), *Review of wave energy technologies and the necessary power-equipment*. Renewable and Sustainable Energy Reviews, Vol.27, p.413–434. https://doi.org/10.1016/J.RSER.2013.07.009

3- Falcão, A.F.O. and Henriques, J.C.C., (2016), *Oscillating-water-column wave energy converters and air turbines: A review*. Renewable Energy, Vol.85, p.1391–1424. https://doi.org/10.1016/J.RENENE.2015.07.086

4- Ashlin, S.J., Sundar, V. and Sannasiraj, S.A., (2016), *Effects of bottom profile of an oscillating water column device on its hydrodynamic characteristics*. Renewable Energy, Elsevier. Vol. 96, p.341–353.

5- Evans, D. V., (1978), *The oscillating water column wave energy device*. Journal Inst Maths Applics, Vol. 22, p.423–433.

6- Falcão, A.F. de O. and Sarmento, A., (1980), *Wave generation by a periodic surface pressure and its application in wave-energy extraction*. 15th International Congress of Theoritical and Applied Mechanics,.

7- Falnes, J. and McIver, P., (1985), *Surface wave interactions with systems of oscillating bodies and pressure distributions*. Applied Ocean Research, Vol.7 (4), p.225–234. https://doi.org/10.1016/0141-1187(85)90029-X

8- Sarmento, A.J.N.A. and De Falcao, A.F.O., (1985), *Wave generation by an oscillating surface-pressure and its applications in wave energy extraction*. Journal of Fluid Mechanics, Vol.150, p.467–485. https://doi.org/10.1017/S0022112085000234

9- Evans, D., (1982), *Wave power absorption by systems of oscillating surface pressure distributions*. Journal of Fluid Mechanics, Vol.114, p.481–499.

10- Brito-Melo, A., Sarmento, A.J.N. a., Clement, A.H. and Delhommeau, G., (1999), *A 3D boundary element code for the analysis of OWC wave-power plants*. Proceedings of the 1999 Ninth International Offshore and Polar Engineering Conference (Volume 1), Brest, France, 30 May - 4 June 1999, Vol.I, p.188–195.

11- Delauré, Y. and Lewis, A., (2003), *3D*

hydrodynamic modelling of fixed oscillating water column wave power plant by a boundary element methods. Ocean Engineering, Vol.30, p.309–330. https://doi.org/10.1016/S0029-8018(02)00032-X

12- Iturrioz, A., Guanche, R., Lara, J.L., Vidal, C. and Losada, I.J., (2015), *Validation of OpenFOAM® for Oscillating Water Column three-dimensional modeling*. Ocean Engineering, Vol.107, p.222–236. https://doi.org/10.1016/j.oceaneng.2015.07.051

13- Vyzikas, T., Deshoulières, S., Giroux, O., Barton, M. and Greaves, D., (2017), *Numerical study of fixed Oscillating Water Column with RANS-type two-phase CFD model*. Renewable Energy, Vol.102, p.294–305. https://doi.org/10.1016/j.renene.2016.10.044

14- Simonetti, I., Cappietti, L., Elsafti, H. and Oumeraci, H., (2017), *Optimization of the geometry and the turbine induced damping for fixed detached and asymmetric OWC devices: A numerical study*. Energy, Elsevier B.V. Vol.139, p.1197–1209. https://doi.org/10.1016/j.energy.2017.08.033

15- Simonetti, I., Cappietti, L., Elsafti, H. and Oumeraci, H., (2018), *Evaluation of air compressibility effects on the performance of fixed OWC wave energy converters using CFD modelling*. Renewable Energy, Elsevier B.V. Vol.119, p.741–753. https://doi.org/10.1016/j.renene.2017.12.027

16- Kamath, A., Bihs, H. and Arntsen, Ø.A., (2015), *Numerical investigations of the hydrodynamics of an oscillating water column device*. Ocean Engineering, Vol.102, p.40–50. https://doi.org/10.1016/j.oceaneng.2015.04.043

17- Morris-Thomas, M.T., Irvin, R.J. and Thiagarajan, K.P., (2007), *An Investigation Into the Hydrodynamic Efficiency of an Oscillating Water Column*. Journal of Offshore Mechanics and Arctic Engineering, Vol.129(4), p.273. https://doi.org/10.1115/1.2426992

18- Luo, Y., Nader, J.-R., Cooper, P. and Zhu, S.-P., (2014), *Nonlinear 2D analysis of the efficiency of fixed Oscillating Water Column wave energy converters*. Renewable Energy, Vol.64, p.255–265. https://doi.org/10.1016/J.RENENE.2013.11.007

19- Anbarsooz, M., Faramarzi, A. and Ghasemi, A., (2016), *A numerical study on the performance of fixed oscillating water column wave energy converter at steep waves*. ASME 2016 Power Conference Collocated with the ASME 2016 10th International Conference on Energy Sustainability and the ASME 2016 14th International Conference on Fuel Cell Science, Engineering and Technology.

20- Elhanafi, A., Fleming, A., Macfarlane, G. and Leong, Z., (2017), *Underwater geometrical impact on the hydrodynamic performance of an offshore oscillating water column–wave energy converter*. Renewable Energy, Elsevier Ltd. Vol.105, p.209–231. https://doi.org/10.1016/j.renene.2016.12.039

21- Elhanafi, A., Macfarlane, G., Fleming, A. and Leong, Z., (2017), *Investigations on 3D effects and correlation between wave height and lip submergence of an offshore stationary OWC wave energy converter*. Applied Ocean Research, Elsevier B.V. Vol.64, p.203–216. https://doi.org/10.1016/j.apor.2017.03.002

22- Elhanafi, A., Macfarlane, G., Fleming, A. and Leong, Z., (2017), *Scaling and air compressibility effects on a three-dimensional offshore stationary OWC wave energy converter*. Applied Energy, Elsevier Ltd. Vol.189, p.1–20. https://doi.org/10.1016/j.apenergy.2016.11.095

23- Elhanafi, A. and Kim, C.J., (2018), Experimental and numerical investigation on wave height and power take–off damping effects on the hydrodynamic performance of an offshore–stationary OWC wave energy converter. Renewable Energy, Vol.125, p.518–528. https://doi.org/10.1016/j.renene.2018.02.131

24- Elhanafi, A., Fleming, A., Macfarlane, G. and Leong, Z., (2017), Numerical hydrodynamic analysis of an offshore stationary–floating oscillating water column–wave energy converter using CFD. International Journal of Naval Architecture and Ocean Engineering, Elsevier Ltd. Vol.9(1), p.77–99. https://doi.org/10.1016/j.ijnaoe.2016.08.002

25- Elhanafi, A., Fleming, A., Macfarlane, G. and Leong, Z., (2016), Numerical energy balance analysis for an onshore oscillating water column--wave energy converter. Energy, Elsevier. Vol.116, p.539–557.

26- Zabihi, M., Mazaheri, S. and Namin, M.M., (2018), Experimental Study of Wave Spectrum Type Impact on Inner Chamber Fluctuation , Pressure and Reflection of OWC Device. INTERNATIONAL JOURNAL OF COASTAL AND OFFSHORE ENGINEERING, Vol.2(3), p.19–27.

27- Zabihi, M., Mazaheri, S. and Montazeri, M.M., (2019), *Experimental hydrodynamic investigation of a fixed o ff shore Oscillating Water Column device*. Applied Ocean Research, Vol.85, p.20–33. https://doi.org/10.1016/j.apor.2019.01.036

28- Hirt, C.W. and Nichols, B.D., (1981), *Volume of fluid (VOF) method for the dynamics of free boundaries*. Journal of Computational Physics, Elsevier. Vol.39(1), p.201–225.

29- Elhanafi, A., Fleming, A., Leong, Z. and Macfarlane, G., (2017), *Effect of RANS-based turbulence models on nonlinear wave generation in a two-phase numerical wave tank*. Progress in Computational Fluid Dynamics, an International Journal, Inderscience Publishers (IEL). Vol.17(3), p.141–158.